Talanta 252 (2023) 123833

Contents lists available at ScienceDirect

Talanta

journal homepage: www.elsevier.com/locate/talanta

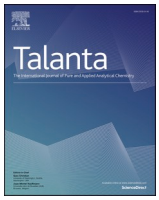

An autonomous synthetic DNA machine for ultrasensitive detection of *Salmonella typhimurium* based on bidirectional primers exchange reaction cascades

Qianru Li [a], Manru Zhang [b], Qingxin Zhang [a], Zhixue Zhu [c], Zhiqiang Guo [d], Jingjing Li [c], Wanqing Xu [c], Jingru Zhu [c], Yuying Yao [c], Zongqiang Li [c], Yu Wang [c], Jiadong Huang [c,d], Su Liu [a,*]

[a] School of Water Conservancy and Environment, University of Jinan, Jinan, 250022, PR China
[b] Shandong Institute of Medical Device and Pharmaceutical Packaging Inspection, Jinan, 250101, PR China
[c] School of Biological Sciences and Technology, University of Jinan, Jinan, 250022, PR China
[d] Key Laboratory of Chemical Sensing & Analysis in Universities of Shandong, School of Chemistry and Chemical Engineering, University of Jinan, Jinan, 250022, PR China

ARTICLE INFO

Keywords:
DNA arch Bridge
Bidirectional primer exchange reaction
Bacteria detection
Fluorescent biosensor
Isothermal amplification

ABSTRACT

Statistics show that food poisoning caused by *Salmonella typhimurium* (*S. Typhimurium*) often tops the list of bacterial food poisoning types in countries around the world. However, detecting traces of *S. Typhimurium* in real samples remains challenging. In recent years, primer exchange reaction (PER), a new isothermal amplification strategy, has rapidly attracted the attention of researchers in the field of biosensing. In this work, We developed a nanostructure called DNA arch bridge (DAB) and combined the DAB with cascade PER technology to construct a novel bidirectional PER (B-PER) for ultra-sensitive detection of pathogenic bacteria as a novel fluorescent biosensor. This strategy relies on the B-PER reaction mediated by binding of the target and adaptor, which occurs with the assistance of Klenow Fragment (KF) (3′-5′exo) polymerase and produces a good deal of G-quadruplex sequences that generate a fluorescent signal by embedding fluorescent dyes. Under the best conditions, the biosensor achieves ultrasensitive detection of *S. Typhimurium*, and the detection limit of the strategy is 9.3 cfu mL^{-1} over the linear detection scope of 10^1-10^5 cfu mL^{-1}. The method has the merits of facile operation, rapid response, and high sensitivity. Furthermore, the biosensor is expected to achieve ultrasensitive detection of various small molecules through recognizing different target and primer sequences. Therefore, our proposed strategy provides an efficient, stable, universal, and practical sensing platform for pathogen and other small molecules detection.

1. Introduction

Pathogenic infection is a major threat to public health because it causes many costly outbreaks around the world every year [1]. Based on the World Health Organization (WHO), foodborne pathogens cause approximately 600 million illnesses and 420,000 deaths annually [2]. *Salmonella typhimurium* (*S. Typhimurium*) is the main cause of bacterial foodborne illness in humans of animal origin. Poultry and swine products are considered the primary carriers of pathogenic *S. Typhimurium*, but the pathogen can be found in meat, eggs, milk, cheese, vegetables, and ready-to-eat products, including nuts and seeds [3–5]. Therefore, rapid, sensitive, specific, and pathogenic cross-validation detection is of vital importance for disease prevention and control of human health [6].

Plate counting is the “gold standard” for bacteria detection within 4–5 days worldwide, including complex pre-enrichment, selective enrichment, separation, and biochemical identification [7]. In recent years, the commonly used detection methods of *S. Typhimurium* include bacterial culture [8], ELISA [9], polymerase chain reaction (PCR) [10], surface-enhanced Raman scattering (SERS) [11], and graphene electrochemical immunosensor [12], etc. Nevertheless, these methods usually have some disadvantages, including time-consuming experimental operation, sophisticated and expensive equipment, and the need for

* Corresponding author.
E-mail address: stu_lius@ujn.edu.cn (S. Liu).

https://doi.org/10.1016/j.talanta.2022.123833
Received 4 May 2022; Received in revised form 13 July 2022; Accepted 7 August 2022
Available online 13 August 2022

well-trained technicians. Hence, there is in dire need to exploit low-budget, simple, high sensitivity, and high specificity detection methods for pathogenic bacteria.

In this context, various colorimetric methods [13], electrochemiluminescence [14,15], and fluorescence [16,17] have been applied to the detection of foodborne pathogens. To improve the sensitivity of the detection, a variety of amplification strategies have been developed, including rolling circle amplification (RCA) [18–20], hybridization chain reaction (HCR) [21–23], catalytic hairpin assembly (CHA) [24–26], primer exchange reaction (PER) [27,28], etc. Among amplification strategies mentioned above, PER is an emerging isothermal amplification strategy, which was first proposed by Yin's research group and has attracted extensive attention in biosensors and bioimaging [29]. Autonomously synthesized ssDNA can be voluntarily detached from the PER hairpin, making it free and reacting with another primer to start the next cycle of ssDNA synthesis [30]. For instance, Li et al. designed an electrochemical platform and used PER as a signal amplification method for detecting exosomal miRNA [31]. Zhou et al. achieved the detection of kanamycin trace based on synchronous signal amplification of PER and metal-dependent DNAzyme [32]. In addition, PER was also used in bioimaging applications. For example, Kishi et al. combined with PER amplification strategy to achieve multiple amplification imaging of RNA and DNA in cells and tissues [33]. Saka et al. intelligently utilized PER strategy to achieve highly reusable and amplified protein imaging in tissues [34]. Compared with RCA, HCR, CHA, etc., PER only needs a hairpin and a primer to perform specific and rapid signal amplification. Considering these advantages, the construction of a biosensor for pathogenic bacteria detection based on PER strategy is worthy of further research.

Herein, we developed a nanostructure called DNA arch bridge (DAB) and combined the DAB with cascade PER technology to construct a novel bidirectional PER (B-PER) for ultra-sensitive detection of pathogenic bacteria as a novel fluorescent biosensor. Our strategy has several important features. First, in our design, the trigger strand T is enclosed by the *S. Typhimurium* aptamer, and the target can bind to its nucleic acid aptamer sequence when the target is present, releasing the T strand. Secondly, We focused on designing a "bridge-like" nanostructure DAB, where the trigger strand T can first grow a new primer sequence T_0 along the right end b part of the DAB using the 3′-5′ extension property of KF polymerase and detach it from H autonomously, T_0 then binds to the left a portion of DAB and triggers the autonomous synthesis of many human telomerase sequences TTAGGG, which repeats to form G-quadruplexes. Finally, thioflavin T (ThT) dye was embedded in G-quadruplex sequences to produce a strong fluorescence signal. In this scheme, the aptamer sequence in the arched probe designed can efficiently recognize the target, thus releasing a large number of trigger chains, and we can also replace the *S. Typhimurium* aptamer by changing the corresponding aptamer to recognize the target as a general-purpose biosensor. At the same time, we have designed and implemented the use of DAB nanostructure to achieve the amplification of the target object, which improves the stability and detection efficiency of the strategy. Therefore, the biosensor is capable of achieving trace detection of *S. Typhimurium* and can also provide a stable, versatile, and efficient biosensing platform for trace molecules in bioanalysis.

2. Experimental section

2.1. Materials and reagents

All DNA fragments shown in Table 1 were purified by HPLC and synthesized by Sangon Biotechnology. Co. Ltd. (Shanghai, China). S1 and S2 form the DNA arch bridge. *S. Typhimurium* (KCTC 1925), *Escherichia coli* (KCTC 2571), *Listeria* (KCTC 3569) and *Bacillus subtilis* (KCTC 1028) were provided from the Institute of Microbiology Chinese Academy (Beijing, China). Peptone, beef extract power, bacto-yeast extract and bacto-tryptone were purchased from Qingdao Biological Technology. Co. Ltd (Qingdao, China).

Table 1
DNA oligonucleotides sequences were used in this work.

Oligonucleotide name	Sequence (5′ to 3′) description
Aptamer (Apt)	**AGTAA TGCCC G**GTAG TTATT CAAAG ATGAG TA**GGA AAAGA**
Trigger (T)	**TCTTTTCC**AAAA**CGGGCATTACT**
S1	**TTAGGGCCCGG**TTTTTT**GGGGGCCCTAACC**AGTAATGC-inverted dT
S2	**GGTTAGGGCCCCC**TTTTTT**CCGGGCCCTAA**CCCTAACC-inverted dT

Klenow Fragment (KF) (3′-5′exo), deoxynucleotides (dATP, dTTP and dGTP) were purchased from New England Biolabs, Inc. The thioflavin T (ThT) was obtained from Sigma-Aldrich Company (Beijing, China). 10 × TBE buffer, DNA Marker, and GelRed were purchased from thermos fisher Co., Ltd. (Beijing, China). N, N, N'N′-tetramethylene diamine (TEMED), ammonium persulfate (AP), and 30% acrylamide solution (29:1) were purchased from Sangon Biotechnology Co., Ltd. (Shanghai, China). All reagents were of analytical grade and used without further purification. Ultrapure water obtained from a Millipore Milli-Q water purification system was used throughout.

2.2. Apparatus

Fluorescence spectra by Agilent Cary Eclipse Spectrophotometer (Agilent, USA) at 425 nm excitation. The excitation and emission slits were set to 5 nm. The fluorescence curve was measured within the scope of 450 nm–600 nm. Polypropylene gel electrophoresis (PAGE) was first performed with the DYCZ-24DN electrophoresis apparatus (LIUYI, Beijing, China), followed by 2 × Gel Red, WD-9405F decolorization Shaker (LIUYI, Beijing, China) shake staining was finally done with Bio-Rad gel imaging system (Bio-Rad, USA).

2.3. Cultivation of strains

All pathogenic strains were incubated in the Luria-Bertani medium at 37 °C for 12 h. The bacterial cells were washed twice with phosphate-buffered saline (PBS, 10 mM, pH 7.4) using a centrifuge at 3000 rpm for 5 min to obtain a logarithmic growth phase. The precipitate was then re-suspended in PBS solution to get the homogeneous suspension of cells. Finally, quantification of bacterial culture results by measuring absorbance at 600 nm.

2.4. Procedures for S. Typhimurium detection

All samples used for *S. Typhimurium* detection were prepared in NEB buffer 2 reaction buffer (10 mM $MgCl_2$, 1 mM DTT, 50 mM NaCl, 10 mM Tris-HCl, pH = 7.9). The specific process was as follows: Apt-T arched probe and DAB were prepared by the annealing method. Apt (100 μM) and T (100 μM) of the same volume were fully mixed and cultured at 95 °C for 5 min, cooled to room temperature, and stored at −20 °C for backup. S1 (3 μL, 100 μM) and S2 (3 μL, 100 μM) and NEB buffer 2 (3 μL,10 ×) were added in 21 μL ultrapure water. The mixture was heated to 95 °C and kept this temperature for 5 min, cooled to room temperature, and stored at −20 °C for backup. Afterwards, Apt-T arched probe (7.5 μL, 40 μM), DAB (3 μL, 10 μM), Klenow Fragment (3′-5′exo) (3 μL, 5000 U/mL), 10 mM dNTPs (10 mM each of dGTP, dTTP, dATP) and ThT (4.5 μL, 100 μM) were taken and reacted at 37 °C for 2h. In the end, the (30 μL) reaction solution was mixed with 70 μL ultrapure water and scanned by an Agilent Cary Eclipse fluorescence spectrometer. All experiments on *S. Typhimurium* measurements were repeated three times in the absence of special instructions.

2.5. PAGE experiment

B-PER amplification products were characterized by 12% PAGE. In the page assay, DNA samples were mixed with DNA loading buffer (volume ratio: 5:1) and subjected to PAGE at 120 V for 70 min in 1 × TBE buffer (pH 8.0). The gel was then stained in 1 × GelRed solution for 30 min, followed by fluorescence detection using the Bio-Rod Gel imaging system.

3. Results and discussion

3.1. Principle of detection of foodborne pathogens based on B-PER sensing strategy

The principle of ultra-sensitive and highly specific fluorescence sensing strategy triggered by the B-PER amplification principle for the detection of foodborne pathogens in Scheme 1. *S. Typhimurium* was selected as the model analyte. The biosensing system includes an arched probe for targeting *S. Typhimurium* consisting of an aptamer and a trigger (T) of *S. Typhimurium*, the DAB for the B-PER amplification response, and KF polymerase, and thioflavin T (ThT). There are four main processes. First, when *S. Typhimurium* was present, specific recognition of the aptamer results in the release of the T chain, and the released T chain can participate in subsequent reactions as a primer chain. Secondly, the released T chain was hybridized with the b portion of the right end of DAB, and simultaneously acted as a primer. When KF polymerase and dNTPs were present, a primer exchange reaction occurred and amplification was terminated at the stop site, thus releasing a new trigger chain (T_0), and DAB was recycled. It is worth noting that we designed the stop site to be controlled using three nucleotides dATP, dGTP, dTTP, which stop amplification due to the lack of cytosine (C) when amplifying to guanine (G) of the template, while the 3′ ends of DAB were modified with inverted-dT to prevent its amplification. Furthermore, the released T_0 chain can hybridize with the portion of the left end of DAB and act as a primer to undergo primers exchange reactions, thereby growing G-quadruplex motifs formed by repeats of the human telomerase sequence TTAGGG, and DAB was recycled. In the end, these G-quadruplex sequences and the organic thioflavin T (ThT) dye interact with each other to produce significantly enhanced fluorescence. Therefore, the amplification strategy based on B-PER has great potential to provide a fast, easy-to-operate, ultrasensitive detection tool for *S. Typhimurium*.

3.2. Feasibility analysis of the constructed biosensor

We verified the feasibility of a B-PER reaction-based biosensor to detect *S. Typhimurium* through a battery of control experiments, the results are placed in Fig. 1. After the addition of *S. Typhimurium*, there was a clearly intense peak at 485 nm, attesting that the fluorescent dye ThT binds to a mass of G-quadruplexes (curve a). By comparison, we found negligible peaks in blank samples, indicating that almost no G-quadruplex were produced (curve b). These data suggest that

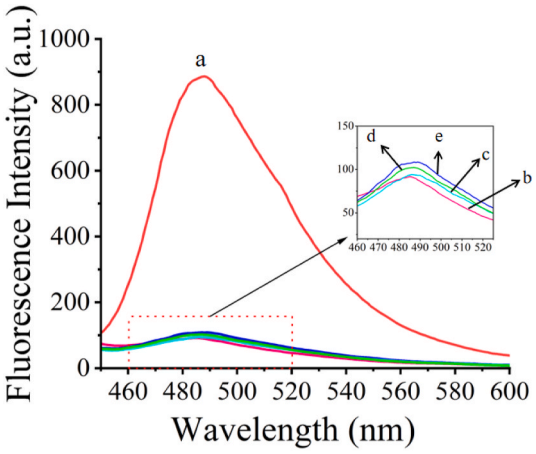

Fig. 1. Fluorescence emission spectrum response of biosensor in the presence of 1×10^5 cfu mL^{-1} *S. Typhimurium* (a). Curves b to f were used for controlled trials in the absence of *S. Typhimurium* (b), KF (c), dNTP (d), and non-target pathogenic bacteria *E. coli* in place of *S. Typhimurium* (e).

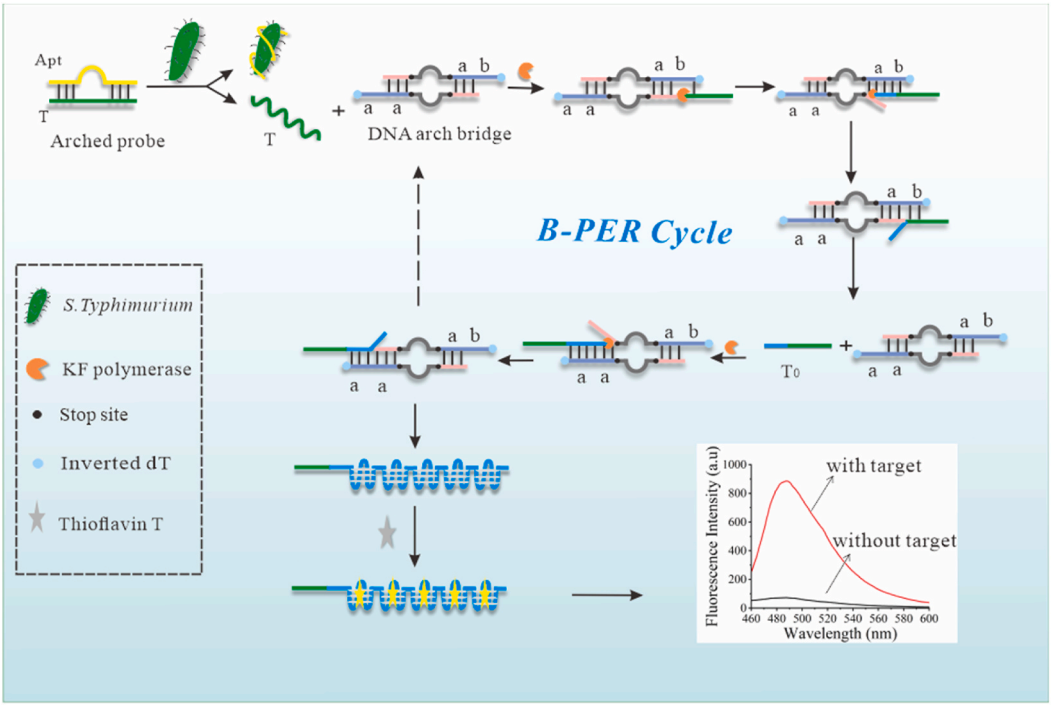

Scheme 1. Schematic diagram of B-PER cascades-based DNA machine for *S. Typhimurium* detection.

S. Typhimurium is capable of specific recognition with the aptamer and initiates the B-PER reaction mediated by KF polymerase, followed by the release of a distinct fluorescence upon ThT fuel embedding. In the absence of KF polymerase in the system, we see a feeble signal similar to that of the blank sample, indicating that the B-PER amplification was assisted by KF polymerase activation (curve c). When no dNTP was present, a weak signal was obtained after incubating with *S. Typhimurium*, indicating that dNTP is essential in the formation of the G-quadruplex sequences (curve d). In addition, when the non-target pathogen *E. coli* replaced *S. Typhimurium*, a quite feeble fluorescence signal was observed, demonstrating that the specific interaction of the target bacteria with the aptamer triggered a significantly enhanced fluorescent signal (curve e). To sum up, the constructed sensor strategy can be used for quantitative analysis of *S. Typhimurium*.

3.3. Gel electrophoresis characterization of fluorescence sensing strategy based on B-PER

Gel electrophoresis analysis can more intuitively observe the reaction mechanism of the biosensor, the results are displayed in Fig. 2. Lane M was a DNA marker of different molecular weights. We verified the specific binding of the target to aptamer shown in Fig. 2A, where lane 1 represents the arched probe prepared by the *S. Typhimurium* aptamer and trigger chain T, Lane 2 was the result of incubation of the arched probe with the target *S. Typhimurium*, and a significant decrease in the brightness of the bands at the location of the arched probe indicates that *S. Typhimurium* and its aptamer bind with the expected specificity. As shown in Fig. 2B, lanes 1, 2 were the bands corresponding to the arched probe and DAB respectively. When *S. Typhimurium* and arched probe were incubated with DAB, KF polymerase, and dNTPs, a clear pathway band (lane 3) appeared on the image, indicating the occurrence of B-PER reaction and the production of a large number of B-PER products with G-quadruplex sequences. In contrast to the absence of a pathway (lane 4) in the arched probe and DAB in blank samples, these data demonstrate that the aptamer in the arched probe specifically binds to *S. Typhimurium* and releases the triggering chain T to trigger the subsequent B-PER response. Lane 5 and 6 were lack of KF polymerase and dNTPs reaction system, we can observe, lanes 5, 6 and blank sample results, indicating the adapter body target-specific binding of T chain after the release because KF polymerase and under the mutual combination of dNTPs B-PER reaction can proceed smoothly, the lack of anyone among them, the work won't completed. The formation of DAB as an important constituent step and component was further verified by electrophoresis. As shown in Fig. 2C, Lanes 1 and 2 were the S1 and S2 chains respectively, and lane 3 was the DAB structure. We can see that the S1 and S2 chains can be well hybridised, suggesting that instead of forming a hairpin structure, S1 and S2 form a DAB structure. This suggests that the whole B-PER process is triggered by the DAB structure.

3.4. Optimization of experimental conditions

To obtain the optimal analytical capability of the B-PER based biosensor for ultra-sensitive detection of *S. Typhimurium*, the reaction time of B-PER reaction, the concentration of KF polymerase, the concentration of arched probe, and the concentration of ThT were studied (Fig. 3). In general, the reaction time was critical to the efficiency of the sensing strategy of B-PER reaction. Therefore, the reaction time was optimized based on the fluorescence intensity of 1×10^5 cfu mL^{-1}. We investigated the change of fluorescence intensity at 485 nm with reaction time (Fig. 3A). The results indicated that the fluorescence intensity of positive samples enhance gradually as time flew, and reached a maximum value at 2h, while the extension of reaction time did not change this value significantly, and the blank samples hardly changed. Therefore, the reaction time of 2h was the best in subsequent experiments. In addition, the ThT concentration of fluorescent dye also has a great influence on fluorescence intensity. We also investigated the variation of fluorescence intensity with ThT concentration in the reaction system, and the result is shown in Fig. 3B. The fluorescence intensity of positive samples increased with increasing ThT concentration and reached balance at a concentration of 15 μM, while the sample intensity of blank samples remained unchanged (Fig. 3B). Thus, we chose 15 μM as the optimal ThT concentration. In addition, specific binding of the aptamer in the arched probe and the target to release the T chain was required to trigger the subsequent reaction, and KF polymerase in the reaction is crucial, so detecting the presence of 1×10^5 cfu mL^{-1} of *S. Typhimurium* $(F - F_0)/F_0$ value to study the arched probe concentration and the concentration of the KF polymerase, the results are shown in fig C and D. The $(F–F_0)/F_0$ value gradually increased increasing arched probe concentration and barely changed at 10 μM (Fig. 3C), so 10 μM was used for the arched probe concentration in subsequent studies. Similarly, the optimized KF polymerase concentration of 0.5 U/μL can be seen in Fig. 3D.

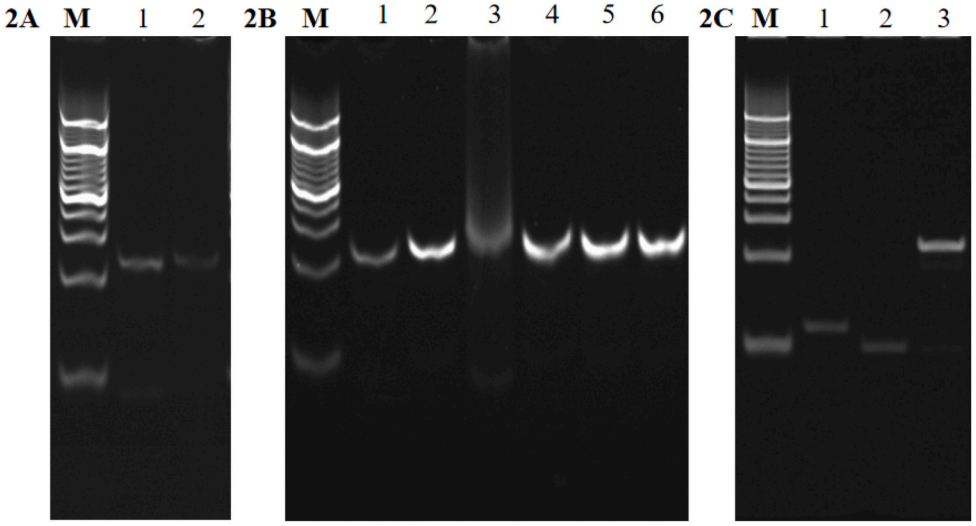

Fig. 2. Gel electrophoresis image of B-PER reaction. Fig. 2A: Lane M, DNA marker; Lane 1, arched probe; Lane 2, arched probe incubated with *S. Typhimurium*; Fig. 2B: Lane M, DNA marker; Lane1, arched probe; lane 2, DAB; Lane 3, positive sample; Lane 4, blank sample; Lane 5, *S. Typhimurium* incubated with Arched probe, DAB and dNTPs; Lane 6, Arched probe incubated with H and KF polymerase; Fig. 2C: Lane M, DNA marker; Lane1, S1; Lane 2, S2; lane 3, DAB.

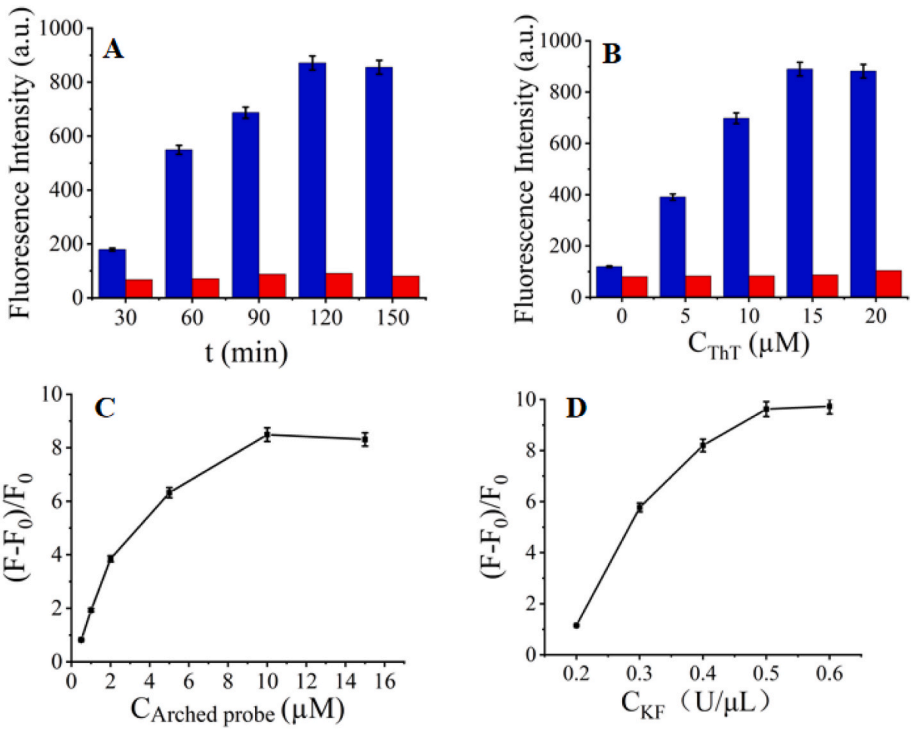

Fig. 3. The optimization of the experimental conditions. (A) The effect of reaction time on fluorescence intensity at 485 nm for the positive samples (blue column) and blank samples (red column); (B) The effect of ThT concentration on fluorescence intensity at 485 nm for the positive samples (blue column) and blank samples (red column); (C) The effect of the concentration of arch probe on the ($F–F_0/F_0$) value, F and F_0 represent the fluorescence intensity at 485 nm in the presence and absence of 1×10^5 cfu mL^{-1} *S. Typhimurium*, respectively; (D) The effect of KF polymerase concentration on the $(F–F_0)/F_0$ value. (For interpretation of the references to color in this figure legend, the reader is referred to the Web version of this article.)

3.5. Analytical performance of S. Typhimurium detection

The detection performance of the constructed biosensor for different concentrations of *S. Typhimurium* was studied by fluorescence spectrometry under optimal conditions. As can be observed from Fig. 4A, the fluorescence intensity at 485 nm at *S. Typhimurium* concentration from 0 to 1×10^5 cfu mL^{-1} increased significantly with increasing concentrations of *S. Typhimurium*. The logarithm of *S. Typhimurium* concentration showed a good linear relationship with fluorescence intensity within the scope of 10^1 cfu mL^{-1}–1.0×10^5 cfu mL^{-1} in Fig. 4B. The linear regression equation was $F = -18.630 + 187.737lgC$ with a correlation coefficient is 0.996. The limit of detection (LOD) for *S. Typhimurium* was calculated to be 9.3 cfu mL^{-1} based on a 3-fold standard deviation rule for the blank response. In addition, we compared this strategy with some existing methods for the quantitative analysis of *S. Typhimurium*. As Table 2 shows, compared with the above methods, the detection limit and detection range of our biosensor are improved to some extent. The ultra-high sensitivity can be attributed to our constructed biosensor based on DAB nanostructures with a B-PER amplification strategy, therefore, our biosensor is feasible.

3.6. Detection specificity

The specificity of constructed sensing strategy was a very important parameter when applied in practice to complex samples. The specificity of the biosensor was verified by the analysis of target *S. Typhimurium* and several non-target foodborne pathogens such as *E. coli*, *Listeria* and *Bacillus*. In Fig. 5, as expected, there was a strong fluorescence signal only present when *S. Typhimurium* is contained, while the fluorescence response to several non-target bacteria was almost identical to that of the blank sample. Experimental results clearly confirmed that the constructed biosensor has outstanding specificity for *S. Typhimurium* detection.

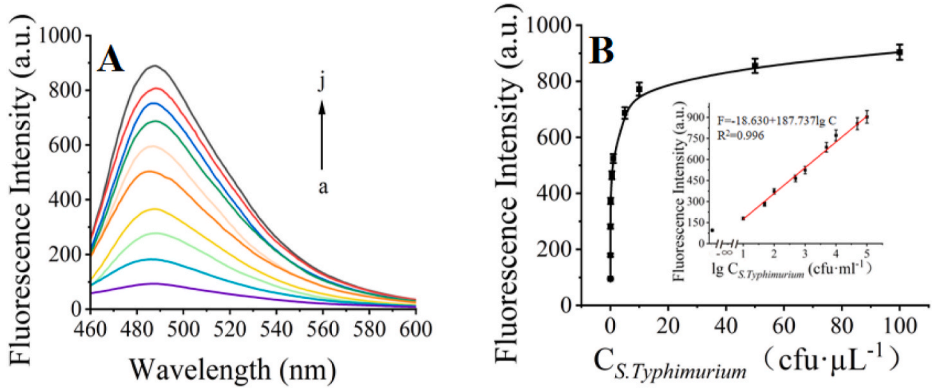

Fig. 4. (A) Response of fluorescence spectra to different concentrations of *S. Typhimurium* (from curves a to j: 0, 10, 50, 1.0×10^2, 5.0×10^2, 1.0×10^3, 5.0×10^3, 1×10^4, 5×10^4, 1.0×10^5 cfu mL^{-1}). (B) Calibration curves of fluorescence intensity at 485 nm for different *S. Typhimurium* concentrations. Inset is the log of the fluorescence intensity at 485 nm against the concentration of *S. Typhimurium*. The error line shows the standard deviation of three repeated experiments.

Table 2
Comparison of different methods for pathogenic bacteria detection.

Methods	Detection range (cfu/mL)	Detection limit (cfu/mL)	Detection time	Ref.
Electrochemical assay	3.0×10^2–3.0×10^7	100	20 min	[35]
Fluorescence assay	4.6×10^2–4.6×10^7	82	3h 50min	[36]
Microfluidic biosensor	10^2–10^7	63	1.5 h	[37]
P-CLISA	5.1×10^3–1.2×10^6	3.36×10^3	6–8 h	[38]
Colorimetric detection	10^1–10^4	11	2.5 h	[39]
Impendence biosensor	10^1–10^6	10	2 h	[40]
Potentiometric sensor	10^2–10^6	20	1 h	[41]
Fluorescence assay	10^1–10^5	9.33	2 h	This work

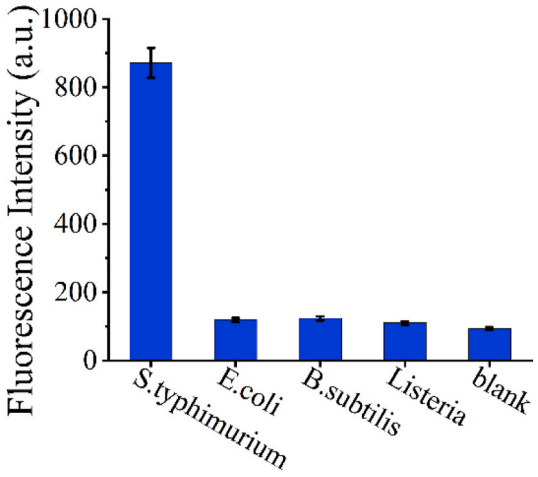

Fig. 5. Fluorescence intensity at 485 nm obtained for the biosensor in the assay of different pathogens. The concentration of *S. Typhimurium* was 1.0×10^5 cfu mL^{-1}. The concentration of non-target bacteria was 1.0×10^6 cfu mL^{-1}. The error bar is the standard deviation of three repeated experiments.

3.7. Application of biosensors in actual samples

We confirmed the practicality of the constructed biosensor by quantifying *S. Typhimurium* in real samples with the spiked method. Different concentrations of *S. Typhimurium* were added to milk samples and determined directly without any pretreatment except for dilution with buffer. As shown in Table 3, the difference between the data obtained by this method and the plate counting method is less, and the differences are less than 5.1%. In addition, the recoveries of milk samples ranged from 99.9% to 107.6%. This clearly proved that our proposed method can be applied to actual sample detection with accuracy and high specificity.

4. Conclusion

In this present study, we constructed a DAB nanostructure, which is a new nanostructure proposed by us. We developed a novel target-triggered B-PER based amplification optical biosensor for ultrasensitive detection of *S. Typhimurium* using DAB nanostructure. Ultrasensitive detection of *S. Typhimurium* in samples by specific recognition of the target and adapter, triggering reusable DAB nanostructure for B-PER reactions. The biosensor has a detection limit of 9.3 for *S. Typhimurium* and a detection range of 4 orders of magnitude, which is better than the majority of existing methods. In addition, compared with the existing methods, this biosensor effectively reduces the non-specific background. Also, based on a B-PER strategy that greatly improves amplification efficiency, our biosensor eliminates the need for sample pretreatment, simplifying the operational steps and allowing for one-step completion. This method has high selectivity for *S. Typhimurium*. It has good recovery and accuracy when used for actual food samples. In general, the biosensor proposed by us has the advantages of high sensitivity, good selectivity, and simple operation. Meanwhile, this strategy with ease extended to other analytes by changing the structure of the aptamer corresponding to the target. Therefore, our newly constructed biosensor may provide a new idea for the detection of food-borne pathogens and other trace molecules.

Table 3
Application of the biosensor in actual samples and comparison with plate counting method.

Spiked amount (cfu/mL)	Found amount (cfu/mL) (±SD, n = 5)		Recovery (%)	
	Our biosensor	Plate count method	Our biosensor	Plate count method
1×10	$(1.011 \pm 0.046) \times 10$	$(0.960 \pm 0.045) \times 10$	101.1	96.1
1×10^2	$(1.001 \pm 0.006) \times 10^2$	$(0.995 \pm 0.004) \times 10^2$	100.1	99.4
1×10^3	$(1.003 \pm 0.015) \times 10^3$	$(0.994 \pm 0.011) \times 10^3$	100.2	99.5
1×10^4	$(0.999 \pm 0.002) \times 10^4$	$(1.004 \pm 0.004) \times 10^4$	99.9	100.4
1×10^5	$(1.077 \pm 0.056) \times 10^5$	$(0.998 \pm 0.027) \times 10^5$	107.6	99.8

Credit author statement

Qianru Li: Methodology, Data curation, Writing – original draft. Manru Zhang: Project administration. Qingxin Zhang: Software, Formal analysis. Zhixue Zhu and Zhiqiang Guo: Data curation. Jingjing Li and Wanqing Xu: Software, Formal analysis. Jingru Zhu, Yuying Yao and Zongqiang Li: Data curation. Yu Wang: Writing - review & editing, Methodology, Funding acquisition. Jiadong Huang: Writing - review & editing, Methodology, Funding acquisition. Su Liu: Writing - review & editing, Methodology, Funding acquisition.

Declaration of competing interest

The authors declare that they have no known competing financial interests or personal relationships that could have appeared to influence the work reported in this paper.

Data availability

Data will be made available on request.

Acknowledgments

This work was supported by the National Natural Science Foundation of China (32072330), Central Government Guides Local Science and Technology Development Projects of Shandong Province (YDZX20203700001955), Jinan City “20 Items in Colleges” Funds (2019GXRC056), and Program for Taishan Scholar of Shandong Province (ts201712048).

References

[1] M.M. Ali, M. Wolfe, K. Tram, J. Gu, C.D.M. Filipe, Y. Li, J.D. Brennan, A DNAzyme-based colorimetric paper sensor for Helicobacter pylori, Angew Chem. Int. Ed. Engl. 58 (29) (2019) 9907–9911, https://doi.org/10.1002/anie.201901873.

[2] H. Yousefi, M.M. Ali, H.M. Su, C.D.M. Filipe, T.F. Didar, Sentinel wraps: real-time monitoring of food contamination by printing DNAzyme probes on food packaging, ACS Nano 12 (4) (2018) 3287–3294, https://doi.org/10.1021/acsnano.7b08010.
[3] J.A. Horlbog, R. Stephan, M.J.A. Stevens, G. Overesch, S. Kittl, M. Napoleoni, V. Silenzi, M. Nuesch-Inderbinen, S. Albini, Feedborne Salmonella enterica serovar jerusalem outbreak in different organic poultry flocks in Switzerland and Italy linked to soya expeller, Microorganisms 9 (7) (2021) 1367, https://doi.org/10.3390/microorganisms9071367.
[4] D.H. Shah, X. Zhou, T. Addwebi, M.A. Davis, L. Orfe, D.R. Call, J. Guard, T. E. Besser, Cell invasion of poultry-associated Salmonella enterica serovar Enteritidis isolates is associated with pathogenicity, motility and proteins secreted by the type III secretion system, Microbiology (Read.) 157 (Pt 5) (2011) 1428–1445, https://doi.org/10.1099/mic.0.044461-0.
[5] I. Machado, V. Garrido, L.I. Hernandez, J. Botero, N. Bastida, B. San-Roman, M. J. Grillo, F.J. Hernandez, Rapid and specific detection of Salmonella infections using chemically modified nucleic acid probes, Anal. Chim. Acta 1054 (2019) 157–166, https://doi.org/10.1016/j.aca.2018.12.027.
[6] L. Ma, L. Peng, L. Yin, G. Liu, S. Man, CRISPR-Cas12a-Powered dual-mode biosensor for ultrasensitive and cross-validating detection of pathogenic bacteria, ACS Sens. 6 (8) (2021) 2920–2927, https://doi.org/10.1021/acssensors.1c00686.
[7] Y. Luo, F. Lv, M. Wang, L. Lu, Y. Liu, X. Xiong, A multicolor electrochemiluminescence device based on closed bipolar electrode for rapid visual screening of Salmonella typhimurium, Sensor. Actuator. B Chem. 349 (2021), 130761, https://doi.org/10.1016/j.snb.2021.130761.
[8] W. Wilkins, C. Waldner, A. Rajic, M. McFall, A. Muckle, R.C. Mainar-Jaime, Comparison of bacterial culture and real-time PCR for the detection of Salmonella in grow-finish pigs in Western Canada using a Bayesian approach, Zoonoses Public Health 57 (Suppl 1) (2010) 115–120, https://doi.org/10.1111/j.1863-2378.2010.01365.x.
[9] Z. Ma, X. Yang, Y. Fang, Z. Tong, H. Lin, H. Fan, Detection of Salmonella infection in chickens by an indirect enzyme-linked immunosorbent assay based on presence of PagC antibodies in sera, Foodb. Pathog. Dis. 15 (2) (2018) 109–113, https://doi.org/10.1089/fpd.2017.2322.
[10] P. Jangampalli Adi, J.R. Naidu, B. Matcha, Multiplex quantification of Escherichia coli, Salmonella typhi and Vibrio cholera with three DNA targets in single reaction assay, Microb. Pathog. 110 (2017) 50–55, https://doi.org/10.1016/j.micpath.2017.06.010.
[11] S. Chattopadhyay, P.K. Sabharwal, S. Jain, A. Kaur, H. Singh, Functionalized polymeric magnetic nanoparticle assisted SERS immunosensor for the sensitive detection of S. typhimurium, Anal. Chim. Acta 1067 (2019) 98–106, https://doi.org/10.1016/j.aca.2019.03.050.
[12] R.R.A. Soares, R.G. Hjort, C.C. Pola, K. Parate, E.L. Reis, N.F.F. Soares, E. S. McLamore, J.C. Claussen, C.L. Gomes, Laser-induced graphene electrochemical immunosensors for rapid and label-free monitoring of Salmonella enterica in chicken broth, ACS Sens. 5 (7) (2020) 1900–1911, https://doi.org/10.1021/acssensors.9b02345.
[13] J. Sun, A.R. Warden, J. Huang, W. Wang, X. Ding, Colorimetric and electrochemical detection of Escherichia coli and antibiotic resistance based on a p-benzoquinone-mediated bioassay, Anal. Chem. 91 (12) (2019) 7524–7530, https://doi.org/10.1021/acs.analchem.8b04997.
[14] L. Yang, X. Yin, B. An, F. Li, Precise capture and direct quantification of tumor exosomes via a highly efficient dual-aptamer recognition-assisted ratiometric immobilization-free electrochemical strategy, Anal. Chem. 93 (3) (2021) 1709–1716, https://doi.org/10.1021/acs.analchem.0c04308.
[15] J. Hu, Z. Shen, L. Tan, J. Yuan, N. Gan, Electrochemical aptasensor for simultaneous detection of foodborne pathogens based on a double stirring bars-assisted signal amplification strategy, Sensor. Actuator. B Chem. 345 (2021), https://doi.org/10.1016/j.snb.2021.130337.
[16] J. Chang, W. Lv, Q. Li, H. Li, F. Li, One-step synthesis of methylene blue-encapsulated zeolitic imidazolate framework for dual-signal fluorescent and homogeneous electrochemical biosensing, Anal. Chem. 92 (13) (2020) 8959–8964, https://doi.org/10.1021/acs.analchem.0c00952.
[17] X. Xia, B. Ma, T. Zhang, Y. Lu, M.R. Khan, Y. Hu, C. Lei, S. Deng, Q. He, G. He, K. Zhang, R. Deng, G-Quadruplex-Probing CRISPR-cas12 assay for label-free analysis of foodborne pathogens and their colonization in vivo, ACS Sens. 6 (9) (2021) 3295–3302, https://doi.org/10.1021/acssensors.1c01061.
[18] L. He, X. Yu, R. Huang, L. Jin, Y. Liu, Y. Deng, S. Li, H. Chen, Z. Chen, Z. Li, P. Xiao, N. He, A novel specific and ultrasensitive method detecting extracellular vesicles secreted from lung cancer by padlock probe-based exponential rolling circle amplification, Nano Today 42 (2022), 101334, https://doi.org/10.1016/j.nantod.2021.101334.
[19] H. Zhao, J. Lv, F. Li, Z. Zhang, C. Zhang, Z. Gu, D. Yang, Enzymatical biomineralization of DNA nanoflowers mediated by manganese ions for tumor site activated magnetic resonance imaging, Biomaterials 268 (2021), 120591, https://doi.org/10.1016/j.biomaterials.2020.120591.
[20] X. Gao, X. Teng, Y. Dai, J. Li, Rolling circle amplification-assisted flow cytometry approach for simultaneous profiling of exosomal surface proteins, ACS Sens. 6 (10) (2021) 3611–3620, https://doi.org/10.1021/acssensors.1c01163.
[21] Z. Li, X. Miao, Z. Cheng, P. Wang, Hybridization chain reaction coupled with the fluorescence quenching of gold nanoparticles for sensitive cancer protein detection, Sensor. Actuator. B Chem. 243 (2017) 731–737, https://doi.org/10.1016/j.snb.2016.12.047.
[22] W. Yang, X. Zhou, J. Zhao, W. Xu, A cascade amplification strategy of catalytic hairpin assembly and hybridization chain reaction for the sensitive fluorescent assay of the model protein carcinoembryonic antigen, Mikrochim. Acta 185 (2) (2018) 100, https://doi.org/10.1007/s00604-017-2620-6.
[23] C. Gu, X. Kong, X. Liu, P. Gai, F. Li, Enzymatic biofuel-cell-based self-powered biosensor integrated with DNA amplification strategy for ultrasensitive detection of single-nucleotide polymorphism, Anal. Chem. 91 (13) (2019) 8697–8704, https://doi.org/10.1021/acs.analchem.9b02510.
[24] Y. Wang, A.M.A. El-Aty, G. Chen, H. Jia, X. Cui, L. Xu, Z. Cao, Y. She, F. Jin, Y. Zhang, A. Hacimuftuoglu, S. Lamu, J. Wang, L. Zheng, M. Jin, B.D. Hammock, A competitive immunoassay for detecting triazophos based on fluorescent catalytic hairpin self-assembly, Mikrochim. Acta 189 (3) (2022) 114, https://doi.org/10.1007/s00604-022-05217-5.
[25] Y. Zhang, X. Zhang, B. Situ, Y. Wu, S. Luo, L. Zheng, Y. Qiu, Rapid electrochemical biosensor for sensitive profiling of exosomal microRNA based on multifunctional DNA tetrahedron assisted catalytic hairpin assembly, Biosens. Bioelectron. 183 (2021), 113205, https://doi.org/10.1016/j.bios.2021.113205.
[26] J. Yu, J. Liu, C.B. Ma, L. Qi, Y. Du, X. Hu, Y. Jiang, M. Zhou, E. Wang, Signal-on electrochemical detection for drug-resistant hepatitis B virus mutants through three-way junction transduction and exonuclease III-assisted catalyzed hairpin assembly, Anal. Chem. 94 (2) (2022) 600–605, https://doi.org/10.1021/acs.analchem.1c03451.
[27] Y. Dai, W. Xu, R.A. Somoza, J.F. Welter, A.I. Caplan, C.C. Liu, An integrated multi-function heterogeneous biochemical circuit for high-resolution electrochemistry-based genetic analysis, Angew Chem. Int. Ed. Engl. 59 (46) (2020) 20545–20551, https://doi.org/10.1002/anie.202010648.
[28] J. Zhang, M. He, C. Nie, M. He, Q. Pan, C. Liu, Y. Hu, T. Chen, X. Chu, Biomineralized metal-organic framework nanoparticles enable a primer exchange reaction-based DNA machine to work in living cells for imaging and gene therapy, Chem. Sci. 11 (27) (2020) 7092–7101, https://doi.org/10.1039/D0SC00339E.
[29] J.Y. Kishi, T.E. Schaus, N. Gopalkrishnan, F. Xuan, P. Yin, Programmable autonomous synthesis of single-stranded DNA, Nat. Chem. 10 (2) (2018) 155–164, https://doi.org/10.1038/nchem.2872.
[30] S. Bu, X. Liu, Z. Wang, H. Wei, S. Yu, Z. Li, Z. Hao, W. Liu, J. Wan, Ultrasensitive detection of pathogenic bacteria by CRISPR/Cas12a coupling with a primer exchange reaction, Sensor. Actuator. B Chem. 347 (2021), 130630, https://doi.org/10.1016/j.snb.2021.130630.
[31] X. Li, X. Li, D. Li, M. Zhao, H. Wu, B. Shen, P. Liu, S. Ding, Electrochemical biosensor for ultrasensitive exosomal miRNA analysis by cascade primer exchange reaction and MOF@Pt@MOF nanozyme, Biosens. Bioelectron. 168 (2020), 112554, https://doi.org/10.1016/j.bios.2020.112554.
[32] W. Zhou, L. Xu, B. Jiang, Target-initiated autonomous synthesis of metal-ion dependent DNAzymes for label-free and amplified fluorescence detection of kanamycin in milk samples, Anal. Chim. Acta 1148 (2021), 238195, https://doi.org/10.1016/j.aca.2020.12.070.
[33] J.Y. Kishi, S.W. Lapan, B.J. Beliveau, E.R. West, A. Zhu, H.M. Sasaki, S.K. Saka, Y. Wang, C.L. Cepko, P. Yin, SABER amplifies FISH: enhanced multiplexed imaging of RNA and DNA in cells and tissues, Nat. Methods 16 (6) (2019) 533–544, https://doi.org/10.1038/s41592-019-0404-0.
[34] S.K. Saka, Y. Wang, J.Y. Kishi, A. Zhu, Y. Zeng, W. Xie, K. Kirli, C. Yapp, M. Cicconet, B.J. Beliveau, S.W. Lapan, S. Yin, M. Lin, E.S. Boyden, P.S. Kaeser, G. Pihan, G.M. Church, P. Yin, Immuno-SABER enables highly multiplexed and amplified protein imaging in tissues, Nat. Biotechnol. 37 (9) (2019) 1080–1090, https://doi.org/10.1038/s41587-019-0207-y.
[35] H. Jiang, D. Jiang, X. Liu, J. Yang, A self-driven PET chip-based imprinted electrochemical sensor for the fast detection of Salmonella, Sensor. Actuator. B Chem. 349 (2021), https://doi.org/10.1016/j.snb.2021.130785.
[36] X. Yang, L. Wang, L. Pang, S. Fu, X. Qin, Q. Chen, C. Man, Y. Jiang, A novel fluorescent platform of DNA-stabilized silver nanoclusters based on exonuclease III amplification-assisted detection of Salmonella Typhimurium, Anal. Chim. Acta 1181 (2021), 338903, https://doi.org/10.1016/j.aca.2021.338903.
[37] F. Huang, R. Guo, L. Xue, G. Cai, S. Wang, Y. Li, M. Liao, M. Wang, J. Lin, An acid-responsive microfluidic Salmonella biosensor using curcumin as signal reporter and ZnO-capped mesoporous silica nanoparticles for signal amplification, Sensor. Actuator. B Chem. 312 (2020), 127958, https://doi.org/10.1016/j.snb.2020.127958.
[38] C. Zhang, Z. Liu, M. Bai, Y. Wang, X. Liao, Y. Zhang, P. Wang, J. Wei, H. Zhang, J. Wang, H. Wang, Y. Wang, An ultrasensitive sandwich chemiluminescent enzyme immunoassay based on phage-mediated double-nanobody for detection of Salmonella Typhimurium in food, Sensor. Actuator. B Chem. 352 (2022), 131058, https://doi.org/10.1016/j.snb.2021.131058.
[39] L. Wang, X. Huo, L. Zheng, G. Cai, Y. Wang, N. Liu, M. Wang, J. Lin, An ultrasensitive biosensor for colorimetric detection of Salmonella in large-volume sample using magnetic grid separation and platinum loaded zeolitic imidazolate Framework-8 nanocatalysts, Biosens. Bioelectron. 150 (2020), 111862, https://doi.org/10.1016/j.bios.2019.111862.
[40] F. Huang, L. Xue, W. Qi, G. Cai, Y. Liu, J. Lin, An ultrasensitive impedance biosensor for Salmonella detection based on rotating high gradient magnetic separation and cascade reaction signal amplification, Biosens. Bioelectron. 176 (2021), 112921, https://doi.org/10.1016/j.bios.2020.112921.
[41] P.M. Shaibani, H. Etayash, K. Jiang, A. Sohrabi, M. Hassanpourfard, S. Naicker, M. Sadrzadeh, T. Thundat, Portable nanofiber-light addressable potentiometric sensor for rapid Escherichia coli detection in orange juice, ACS Sens. 3 (4) (2018) 815–822, https://doi.org/10.1021/acssensors.8b00063.